Highly Sensitive Co-trench Detection of Optical Fibers by Correlation Analysis with Field Test

Jiachuan Lin[1], Zhiping Jiang[1]*, Tao Zhang[2], Qingpeng Liu[2], Haiming Qin[2], Hao Li[1]
[1]Ottawa Research Center, Huawei Technologies Canada Co., Ltd., 303 Terry Fox Drive, Kanata, ON, K2K 3J1, Canada
[2] AI Application Development Dept, Huawei Technologies Co., Ltd., Wuhan, 430223, China
*zhiping.jiang@huawei.com

Abstract: A coherent-OTDR and correlation analysis-based method is proposed to detect co-trench fibers. High sensitivity and accuracy are demonstrated in a field test with two partially co-trenched fibers. © 2024 The Author(s)

1. Introduction

In optical networks, a survivability mechanism is to reserve a protection path to detour the data traffic in the event of the primary data path failure. For proper protection, the primary and protection paths are required to be geographically disjoint, as shown in Fig. 1. However, in practice, there are cases of improper protection with the primary and protection paths ending up sharing the same cable, or trench due to inaccurate fiber route information. Therefore, to guarantee proper protection, sensitive and accurate co-cable/co-trench detection scheme is highly desirable [1].

Data-carrying fiber has been proven to be a feasible sensing medium to monitor surrounding events across different application scenarios [2-4]. Using sensing capability of data fibers, with two coherent optical time domain reflectometers (C-OTDRs), it is possible to simultaneously monitor the primary and protection fibers from the remote end. It results in a waterfall diagram for each fiber and the similarity of features/patterns in these two diagrams is an indication of close proximity [5]. However, clear and distinct patterns/features in 2D waterfall diagrams require strong events around the fiber (e.g., a vehicle passing over a buried fiber). With fibers only subject to weak events, the waterfall patterns/features are buried in noise, this method faces challenge.

In this paper, a highly sensitive and accurate scheme based on correlation analysis is proposed. The method is verified using field collected data.

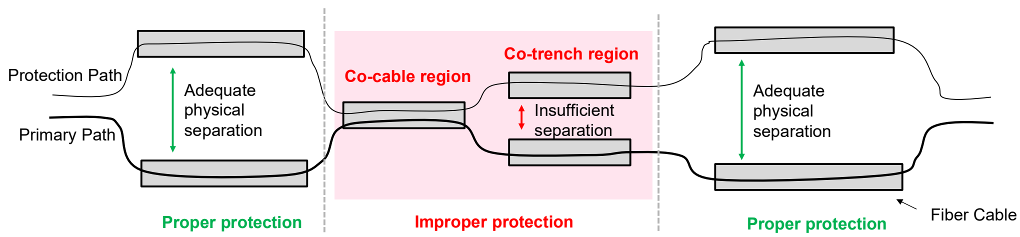

Fig. 1. Illustration of proper/improper protection path.

2. C-OTDRs based Co-trench Analysis

The co-cable/co-trench detection system uses two C-OTDR modules that work simultaneously. The data processing flowchart shown in Fig. 2 includes three steps of pre-processing, time-frequency correlation analysis, and 2D-detection. The captured 2D-traces from fiber-a and fiber-b are denoted as $u_a(t,z)$ and $u_b(t,z)$, where t is the slow time axis (t-axis, sampling rate is the repetition rate of the C-OTDR pulses) and z denotes the distance axis (z-axis, sampling rate is calculated based on the analogy-to-digital converter sampling rate). In the pre-processing stage, $u_a(t,z)$ and $u_b(t,z)$ are normalized and then filtered by a high pass filter (HPF). The HPF is used to select the most effective acoustic frequency components. After pre-processing, we obtain the waveforms $w_a(t,z)$ and $w_b(t,z)$, and they are sent into the correlation analysis module. In the correlation module, the similarity of two selected data sections from two fibers are calculated using time-frequency correlation. The selected two sections start at the locations z_a and z_b respectively. Each section has a distance window length of L and a time window length of T. For each comparison of two selected sections, the calculated correlation coefficient is denoted as $C(z_a, z_b)$. Since the two C-OTDRs are synchronized, the correlation calculation is swept over z-axis only. After sweeping z_a and z_b, the correlation coefficient matrix $C(z_a, z_b)$ is obtained.

To further improve the detection accuracy, we apply a 2D detection over the correlation coefficient matrix $C(z_a, z_b)$, obtaining $D(z_a, z_b)$. The used 2D detection is based on Eq. (1),

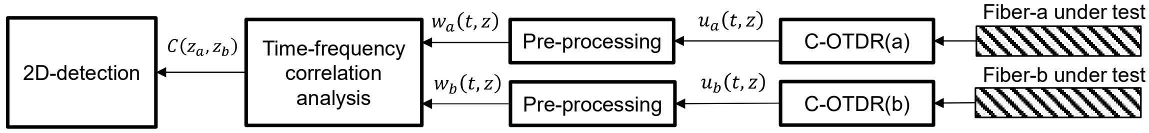

Fig. 2. Data processing flow-chart for co-cable/co-trench analysis.

$$D(z_a, z_b) = \text{mean}(|C(z_a - X, z_b - Y) - R(X, Y)|), \tag{1}$$

where $R(X, Y)$ is the ideal 2D correlation result, and a delta function is used to approximate the ideal one in this work. X, Y are the sample ranges used for the 2D detection calculation. After 2D-detection, the co-cable/co-trench region decision can be made.

3. Field Data Verification and Discussion

The method is verified using field captured data from one path configuration. In the field test, the two fibers have almost the same length of ~10 km. The first ~3.3 km of the two fibers are in the same trench, but not in the same cable, while the rest sections are disjoint. The physical location of tested path is indicated in Fig. 3(a), and the surrounding contains both "quiet" and "noisy" environments. In some sections, the two fibers are buried under Hutong area (quiet zone), with no heavy vehicles travel through; some sections are buried under an urban street, where the vehicles are with moderate speeds; in some sections, the two fibers are placed around 5~10 meters next to an urban highway. Two coarsely synchronized (accuracy on the order of 1 s) C-OTDRs are used to capture the back reflected light, and only vibration magnitude (i.e. distributed vibration sensing, DVS) data is used for co-trench/co-cable analysis.

In the Fig. 3(b), we show one group captured data of 10 km × 1 s waterfall plots of $u_a(t, z)$ and $u_b(t, z)$. The brighter regions indicate strong events (such as vehicle passing), while the dark blue regions are "quiet zones" with weak events. Fig. 3(c)-(e) show the correlation results of $C(z_a, z_b)$ calculated using same distance window length of $L = 100$ m but different time window lengths of T = 1 s, 16 s, and 1088 s. In these plots, the z_a-axis denotes the location of selected section of fiber-a with a step size of 100 m, and the z_b-axis denotes the selected comparison location of fiber-b with a step size of ~10 m. As can be seen, with $T = 1$ s in Fig. 3(a), the diagonal direction does not show a clear co-trench signal. When T increases to 16 s, the brighter dots show up, indicating the potential positive detection results of co-cable/co-trench. As the time window length T keeps increasing to 1088 s, much brighter dots can be seen, covering the first 3.3 km region. After 3.3 km, the correlation results show no significant co-trench signals.

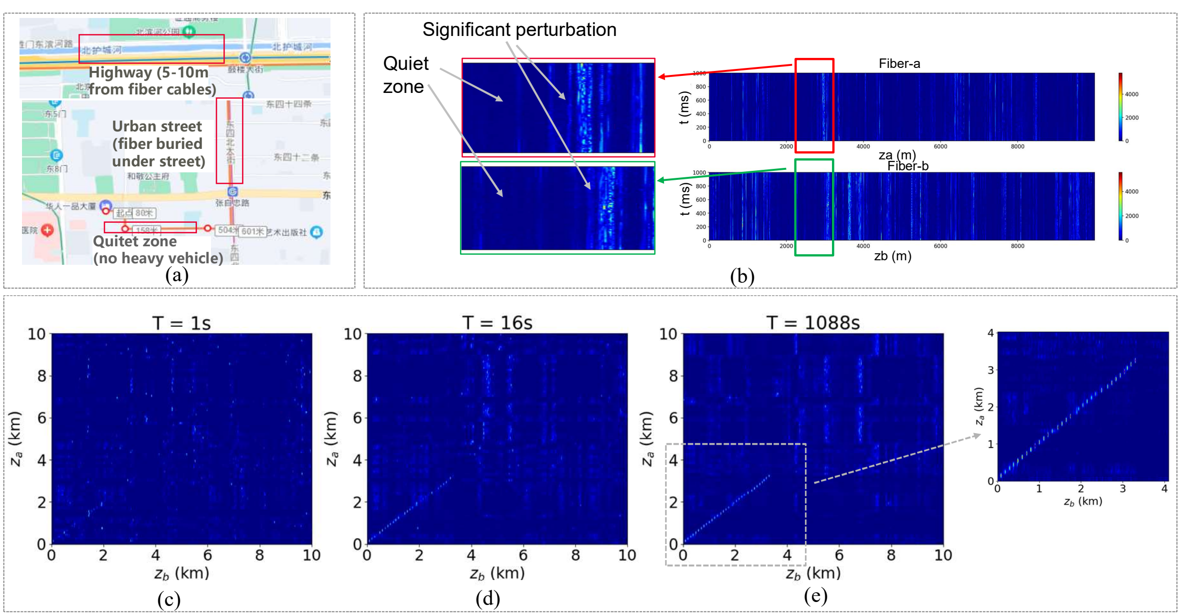

Fig. 3. (a) Illustration of field test link environment; (b) one captured amplitude data of C-OTDRs showing environment with strong events and "quiet zone"; (c)-(e) correlation coefficients calculated using T=1 s, 16 s and 1088 s respectively.

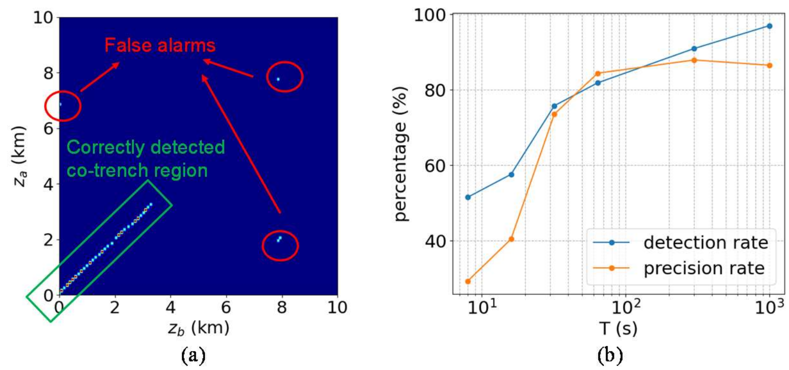

Fig. 4. (a) 2D-detection result of *T*=1088 s; (b) detection rate and precision rate vs. time window length *T*.

Fig. 4(a) shows the example results of applying 2D-detection to $C(z_a, z_b)$ at *T*=1088 s. Based on Fig. 4a, the decision is made and confusion table is extracted, summarized in Tab. 1. In this verification, the comparison/decision is made over a 100×100 matrix, giving total 10,000 sample points. In Tab. 1, there are 32 true positives (TPs, representing correct detection), only 1 false negative (FN, representing missed detection). The FN happened at location near $z_a, z_b = \sim 2$ km, it may be caused by 2D detection. The algorithm mitigates the background noise floor based on the mean value of a certain 2D region, thus it merges two adjacent dots in this section. However, the merged two dots can be visually separated in the zoom-in plot of Fig. 3(e). In the rest two quadrants of Tab. 1, there are 4 false positives (FPs, representing missing alarm) and 9963 correctly detected true negatives (TNs). The FPs happens because there still exists some remaining background noise floor in the results of $C(z_a, z_b)$. Furthermore, the detection rate (DR) and precision rate (PR) are calculated. The DR is defined as $\mathrm{TP}/(\mathrm{TP}+\mathrm{FN})$, and PR is defined as $\mathrm{TP}/(\mathrm{TP}+\mathrm{FP})$. Finally achieving DR = 97% and PR = 88.9%.

Table 1. Confusion table of *T*=1088 s

Confusion Matrix		**Prediction**	
		Positive	**Negative**
Actual	**Positive**	32 (TP)	1 (FN)
	Negative	4 (FP)	9963 (TN)

The performance vs. time window length *T* is also summarized in Fig. 4(b). It can be seen that, when *T*= 60 s, the DR reaches 80%. When *T* increases to 300 s, it reaches 90%. For *T*=1000 s, almost all of co-trench regions are clearly labeled. The precision rate stays around 85% for the tested *T* range. The PR is hard to be further improved as the FPs cannot be fully removed due to the limited capability of current noise suppression algorithm.

4. Conclusion

Using magnitude data of C-OTDR, a correlation analysis based method is proposed to detect the improper protection. The method provides high sensitivity without relying on strong events. A field test, a challenging case of co-trench with quiet surroundings (weak events), shows very accurate detection of improper protection at a high spatial resolution of ~10 m. The detection rate achieved is >95 % by using 1088 s data. Optimization of test time, shared-path resolution can be explored in future work.

References

[1] MW Ashraf, *et al.*, “Disaster-Resilient Optical Network Survivability: A Comprehensive Survey,” MDPI Photonics, vol. 5, no. 4, pp. 35, 2018.
[2] Ting Wang, *et al.*, "Employing fiber sensing and on-premise AI solutions for cable safety protection over telecom infrastructure", in Optical Fiber Communications Conference and Exhibition (OFC), San Diego, CA, USA, 2022, pp. 1-3.
[3] Glenn A. Wellbrock, *et al.*, "First field trial of sensing vehicle speed, density, and road conditions by using fiber carrying high speed data", in Optical Fiber Communications Conference and Exhibition (OFC), San Diego, CA, USA, 2019, pp. 1-3.
[4] Tieyuan Zhu, *et al.*, "Sensing Earth and environment dynamics by telecommunication fiber-optic sensors: An urban experiment in Pennsylvania, USA." Solid Earth, vol. 12, no. 1, pp. 219-235, 2021.
[5] Yunbo Li, *et al.*, "Research and Experiment on AI-based Co-cable and Co-trench Optical Fibre Detection", in European Conference on Optical Communication (ECOC), Basel, Switzerland, 2022, pp. 1-4.
[6] Guojie Tu, *et al.*, "The Development of an Φ-OTDR System for Quantitative Vibration Measurement", IEEE Photonics Technology Letters, vol. 27, no. 12, pp. 1349-1352, 2015.